Clonal evolution of acute myeloid leukemia with *FLT3*-ITD mutation under treatment with midostaurin

Laura K. Schmalbrock *et al.*

Supplemental Methods

Patients and treatment

We included 75 *FLT3*-ITD positive patients who were treated within the RATIFY[1] (NCT00651261; n=25), AMLSG 16-10[2] (NCT01477606; n=41) trials, AMLSG 07-04[3] (NCT00151242; n=7) and AMLSG 11-08[4] (NCT00850382; n=2) trials. As recently published by Stone et al.[1], treatment within the RATIFY trial consisted of induction chemotherapy [60mg/m^2 daunorubicin, day (d) 1-3 / 200mg/m^2 cytarabine, d1-7] in combination with midostaurin (50mg twice a day, d8-21) or placebo. In our study cohort, midostaurin was administered within the RATIFY trial in 13 patients and 12 patients received placebo. Induction therapy was followed by up to 4 cycles of high-dose cytarabine (HDAC; 3000mg/m^2 d1,3,5) in combination with midostaurin (50mg twice a day, d8-21). Allogeneic hematopoietic stem cell transplantation (HSCT) was performed on the investigator's discretion (1 patient in our study cohort). After chemotherapy-based consolidation, 9 patients received a one-year maintenance therapy with midostaurin (50mg twice a day, d1-28).

Within the AMLSG 16-10 trial, all patients received midostaurin [50mg twice a day, d8 until 48 hours (hrs) before the next chemotherapy cycle] during induction chemotherapy (60 mg/m^2 daunorubicin d1-3 / 200 mg/m^2 cytarabine, d1-7). Allogeneic

HSCT was the first priority for consolidation and performed in 8 of the 41 patients. Patients not transplanted in first CR received age-adapted HDAC [3000mg/m^2 (age 18-65 years), d1,3,5; 1000mg/m^2 (age > 65 years), d1,3,5] in combination with midostaurin (50mg twice a day, d6 until 48 hrs before the next chemotherapy cycle). A one-year maintenance therapy with midostaurin (50mg twice a day, d1-28) was intended for all patients, starting after chemotherapy-based consolidation (n=8) or 30 days after HSCT (n=6).

We also included in total n=9 additional patients in the control group which were treated without the addition of midostaurin within the AMLSG 07-04 (n=7) and AMLSG 11-08 (n=1) trials as previously published.[3,4]

Sample preparation

Bone marrow (BM) and peripheral blood (PB) samples obtained at the time of diagnosis, in CR, at relapse / refractory disease were enriched for mononuclear cells by Ficoll gradient centrifugation. Purified cells were frozen at -80°C and DNA and RNA isolated using the AllPrep Mini Kit (Qiagen, Hilden, Germany).

Cytogenetics

For chromosome banding analysis, metaphases of sufficient quality were available in pre-treatment samples for 71 patients. Chromosomal aberrations were described according to the International System for Human Cytogenetic Nomenclature (ISCN) version 2009.

Detection of *FLT3*-ITD at diagnosis, relapse and refractory disease

The presence of *FLT3*-ITD was determined by DNA-based PCR followed by capillary electrophoresis (Genescan-based fragment-length analysis) at the time of

diagnosis and relapse / refractory disease in all patients; sequencing was performed to determine the ITD insertion site as previously described.[1] *FLT3*-ITD was assigned 'negative' if the allelic ratio (AR) was <0.05. *FLT3*-ITDs were characterized at diagnosis, relapse / refractory disease in patients with regard to the number of detectable ITD clones, the nucleotide (nt) length and the ITD insertion site based on functional regions of the FLT3 receptor [juxtamembrane domain (JMD), tyrosine kinase domain 1 (TKD1)].[5]

The ARs at diagnosis and relapse / refractory disease based on Gene-scan analysis was available for all n=75 patients. Information about *FLT3*-ITD length and insertion sites were available for 72/75 patients at diagnosis (Gene-scan n=71, WES n=1) and for 71/75 patients at relapse (Gene-scan n=70, WES n=1).

Whole Exome Sequencing data analysis

For analysis of WES data, paired-end sequences were aligned to the human reference genome hg19 using BWA-MEM[6] after de-multiplexing, followed by sorting and indexing of the BAM files using SortSam and BuildBamIndex (both Picard 1.138, http://broadinstitute.github.io/picard). All PCR duplicates were removed (MarkDuplicates, Picard 1.138) and the initial alignment defined by local re-alignment (Indel Realigner, GATK 3.4-46)[7]. Variants were called using VarScan2[8]. by comparing diagnosis and tumor samples at disease progression to the matching remission sample (patients with relapsed disease) or $CD3^+$ sorted T-cells in patients with refractory disease. Variants were annotated using ANNOVAR[9]. To identify mutations known to persist in remission (*DNMT3A*, *TET2*, *ASXL1*), we applied a custom script for variants in genes known to be recurrently mutated in AML. The remaining variants were filtered for intronic and synonymous variants, variants with less than 2 tumor variant supporting reads in the forward and reverse direction, variants with an entry in data base of single

nucleotide polymorphisms (dbSNP Build ID138, 1000 Genomes Project)[10,11] but not in COSMIC[12] v70 (http://cancer.sanger.ac.uk/cosmic), variants located in segmental duplication areas and variants which are located in polymer-repeat regions. The analysis pipeline is available at https://github.com/tjblaette/ngs. We further defined a variant allele frequency (VAF) of 5% for variant calling due to the sensitivity of the method. Variants not meeting these criteria were included if present in the same patients at a second time point with high confidence. To exclude donor-related variants in relapse samples of patients who relapsed after HSCT, we called only variants 'TRUE' which were present also at diagnosis or were known oncogenic variants. Pathways analysis was performed using gene sets from the Molecular Signatures Database (MSigDB, https://www.gsea-msigdb.org/gsea/msigdb/index.jsp)[13]. We compared mutations between diagnosis and relapse/refractory disease in all patients with respect to midostaurin treatment and *FLT3*-ITD status (+/-) at the time of disease progression.

Validation of recurrent gene mutations

The presence of 42 recurrently AML-associated gene mutations as given in supplemental Table S1 were validated in selected samples with ultra-deep targeted re-sequencing. Samples were processed according to the manufacturer's instructions using a custom designed HaloPlex HS Target Enrichment System (Agilent) with 230.4 ng input gDNA. Sequencing of pooled DNA was performed on an Illumina MiSeq using the MiSeq Reagent Kit v2 (300-cycles, Illumina).

Trimmed sequencing reads were aligned to the human reference genome GRCh37 using BWA-MEM. Deduplication by molecular barcodes was performed with BamDeduplicateByBarcode from ngs-bits followed by sorting and indexing using Picard (Picard 1.138, http://broadinstitute.github/io/picard). GATK (Indel Realigner,

GATK 3.4-46) was used for local realignment. Coverage calculation of alignments was performed with BEDTools. Pileups were generated with SAMtools and VarScan2 used for variant calling. Variants were annotated using ANNOVAR. Filtering was applied for intronic variants, and variants with an entry in dbSNP(138) but not in the COSMIC v70. Variants were manually checked using the Integrative Genomics Viewer (Broad Institute, Cambridge, MA). Due to the sensitivity of our assay, variants with a VAF >3% were considered 'TRUE'. The average coverage of our assay was 600 to 800x.

$CD3^+$ T-cell sorting

Because remission samples were not available for patients with refractory disease, we performed $CD3^+$-based T-cell sorting from diagnostic samples (BM n=2; PB n=17) to obtain normal T-cells as controls for WES.

Viable cells stored at -196 °C were thawed and rapidly collected in pre-warmed (37°C) RPMI media. Cells were washed twice (311xg for 7 minutes) and suspended in 900µl medium. To select for T-cells, we used CD3 MicroBeads (MACS Miltenyi) and performed a positive selection according to the manufacturer's instructions. To increase the specificity of magnetic labeling we added FcR blocking reagent (MACS Miltenyi) to the incubation reaction. Magnetic separation was performed using MS columns for cell counts ≤$2x10^5$ (MACS Miltenyi) or LD columns (MACS Miltenyi) if cell count was >$2x10^5$. To further increase the purity of the $CD3^+$ sorted cells, magnetic separation was performed twice with two washing steps. In each reaction, a control sample was also enriched for T-cells and the purity determined with Fluorescence-activated cell sorting (FACS) according to standard protocols. The purity of $CD3^+$ sorted cells of all controls was >85%. $CD3^+$ enriched cells were immediately stored at -80 °C and DNA isolated using the AllPrep Mini Kit (Qiagen, Hilden, Germany). Low

DNA quantities were amplified using the GenomiPhi V2 DNA Amplification Kit (GE Healthcare) before WES.

Fish Plots

We generated Fish plots to visualize the clonal evolution pattern of mutations over the course of treatment in individual patients. We defined mutation clusters according to the VAFs present at diagnosis and relapsed / refractory disease. Mutation clusters were considered to correspond to a clone if VAFs were similar within a range of ~15% at each time point and showed comparable VAF changes between diagnosis, CR and relapse (e.g. mutations present with comparable VAFs at diagnosis/relapse, mutations that were lost or gained at relapse). For each cluster, a representative VAF was estimated by the median of the cluster mutation VAFs. Clones were considered paternal if the median VAF was higher compared to the representative VAF of subclones or the sum of subclonal representative VAFs at each time point. Based on the parenthood of the so defined mutation clusters and their representative VAFs, Fish plots were generated using the Fish plot package for R.[14]

Analysis of Plasma inhibitory Activity

Plasma inhibitory Activity (PIA) was measured in plasma samples by antiphosphotyrosine immunoblotting as previously described.[15] PIA was calculated for each sample with densitometric analysis by analyzing the respective immunoblot density compared to the percent decrease from the baseline density (100% = no FLT3 inhibition). Data from PIA analysis at the time of diagnosis, after first cycle of induction chemotherapy and at the time of relapse / refractory disease was available for n=12 patients, of which n=6 were *FLT3*-ITD negative and n=6 *FLT3*-ITD positive at relapse / refractory disease.

Statistical analysis

The definitions of CR, relapse / refractory disease were based on recommended criteria.[16] Pairwise comparisons between continuous variables were performed using a non-parametric two-sided t-test (Mann-Whitney test) using the software GraphPad Prism (Version 7.01). Categorical variables were calculated using the Fisher's exact test. An effect was considered significant if the *P* value was .05 or less.

The stability of mutations per patient was calculated by dividing the number of mutations present at both time points (diagnosis and relapse / refractory disease) by the total number of mutations.

References

1. Stone RM, Mandrekar SJ, Sanford BL, et al. Midostaurin plus Chemotherapy for Acute Myeloid Leukemia with a *FLT3* Mutation. *N. Engl. J. Med.* 2017;377(5):454–464.
2. Schlenk RF, Weber D, Fiedler W, et al. Midostaurin added to chemotherapy and continued single-agent maintenance therapy in acute myeloid leukemia with FLT3 -ITD. *Blood*. 2019;133(8):840–851.
3. Schlenk RF, Lubbert M, Benner A, et al. All-trans retinoic acid as adjunct to intensive treatment in younger adult patients with acute myeloid leukemia: results of the randomized AMLSG 07-04 study. *Ann. Hematol.* 2016;95(12):1931–1942.
4. Paschka P, Schlenk RF, Weber D, et al. Adding dasatinib to intensive treatment in core-binding factor acute myeloid leukemia-results of the AMLSG 11-08 trial. *Leukemia*. 2018;32(7):1621–1630.
5. Kayser S, Schlenk RF, Londono MC, et al. Insertion of FLT3 internal tandem duplication in the tyrosine kinase domain-1 is associated with resistance to chemotherapy and inferior outcome. *Blood*. 2009;114(12):2386–2392.
6. H L. Aligning sequence reads, clone sequences and assembly contigs with BWA-MEM. *https://arxiv.org/abs/1303.3997*. 2013;
7. McKenna A, Hanna M, Banks E et al. The genome analysis toolkit: a mapreduce framework for analyzing next-generation DNA sequencing data. *Genome Res.* 2010;20:1297–1303.
8. Koboldt DC, Zhang Q, Larson DE et al. VarScan 2: somatic mutation and copy number alteration discovery in cancer by exome sequencing. *Genome Res.* 2012;22:568–576.
9. Wang K, Li M, Hakonarson H et al. ANNOVAR: functional annotation of

genetic variants from high-throughput sequencing data. *Nucleic Acids Res.* 2010;38:e164–e164.

10. Sherry ST, Ward MH, Kholodov M et al. dbSNP: the NCBI database of genetic variation. *Nucleic Acids Res.* 2001;29:308–311.
11. The 1000 Genomes Project Consortium. A global reference for human genetic variation. *Nature*. 2015;526:68–74.
12. Forbes SA, Beare D, Gunasekaran P et al. COSMIC: exploring the world's knowledge of somatic mutations in human cancer. *Nucleic Acids Res.* 2015;43:D805–D811.
13. Subramanian A, Tamayo P, Mootha VK et al. Gene set enrichment analysis: A knowledge-based approach for interpreting genome-wide expression profiles. *Proc. Natl Acad. Sci. USA.* 2005;102:15545–15550.
14. Miller CA, Mcmichael J, Dang HX, et al. Visualizing tumor evolution with the fishplot package for R. *BMC Genomics*. 2016;16–18.
15. Levis M, Brown P, Smith BD et al. Plasma inhibitory activity (PIA): a pharmacodynamic assay reveals insights into the basis for cytotoxic response to FLT3 inhibitors. *Blood*. 2006;108(10):3477–3483.
16. Döhner H, Estey E, Grimwade D, et al. Diagnosis and management of AML in adults: 2017 ELN recommendations from an international expert panel. *Blood*. 2017;129(4):424–447.
17. Papaemmanuil E, Gerstung M, Bullinger L, et al. Genomic Classification and Prognosis in Acute Myeloid Leukemia. *N. Engl. J. Med.* 2016; 74(23):2209-2221.

Supplemental Tables

Supplemental Table 1. Cytogenetic alterations present at diagnosis in patients treated with or without midostaurin in combination with intensive chemotherapy

No Midostaurin

Study	UPN	Karyotype at diagnosis
RATIFY	1	46,XX
RATIFY	5	46,XX
RATIFY	6	46,XX
RATIFY	7	46,XY
RATIFY	9	46,XX
RATIFY	15	46,XX
RATIFY	19	46,XX
RATIFY	20	46,XY
RATIFY	34	46,XY,del(9)(q13q22);46,XY,del(9)(q13q22),-22,+mar;46
RATIFY	37	46,XX
RATIFY	39	46,XX
RATIFY	41	46, XX
07-04	69	46,XY
07-04	70	46,XX
07-04	71	46,XX
07-04	72	46,XY
07-04	73	46,XX,t(8;21)(q22;q22),del(11)(q21q23),del(14)(q24q32)
07-04	74	46,XX
07-04	75	46,XY
11-08	76	46,XX,t(8;21)(q22;q22)
11-08	77	46,XY

Midostaurin treated

Study	UPN	Karyotype at diagnosis
16-10	2	46,XY,del(3)(p13p14); 46,XY
RATIFY	3	46,XY
RATIFY	4	46,XY
16-10	8	46,XY
RATIFY	10	na
RATIFY	11	na
16-10	12	46,XY
16-10	13	46,XX,t(9;11)(p22;q23)
16-10	14	46,XY,t(6;9)(p23;q34)
16-10	16	46,XY
16-10	18	46,XY
RATIFY	21	46,XY
RATIFY	22	46,XY
RATIFY	23	46,XY,t(6;9;6;9)(p23;q34;q21;q34)
16-10	24	46,XY
16-10	25	46,XY
RATIFY	26	47, XX, +8, 48, XX, +8, +21
16-10	27	46,XX
RATIFY	28	46,XX
16-10	29	46,XY,t(6;9)(p22;q34)
16-10	30	na
16-10	31	46,XX
16-10	32	46,XY
16-10	33	46,XY
16-10	35	46,XY
16-10	38	46,XY
RATIFY	40	46,XY
RATIFY	42	46,XX
16-10	43	46, XY del (20)(q11.2q13.2); 46, idem.iso(8)(q10), +8 der (8;16) (q10;q12); 46, XY
RATIFY	44	46,XX
16-10	45	46,XX
16-10	46	46,XX
16-10	47	46,XY
RATIFY	48	46,XX
16-10	49	46,XY
16-10	50	46,XX
16-10	51	na
16-10	52	46, XY
16-10	53	46,XY; t(6;9)(p22;q34); 46,XY
16-10	54	46,XX
16-10	55	46,XX
16-10	56	46,XX
16-10	57	46,XY
16-10	58	46,XY,t(6;9)(p22;q34); 46,XY
16-10	59	46,XY
16-10	60	46,XX
16-10	61	46,XX
16-10	62	46,XX,t(6;11)(q27;q23)
16-10	63	46,XX
16-10	64	46,XX,t(5;14)(q32;q32)
16-10	65	46,XX,i(14)(q10); 46,idem,t(X;3)(p11;p13)
16-10	66	46,XY
16-10	67	47, XX, +14
16-10	68	46,XX,add(19)(q31.1)

na=not available

Supplemental Table 2. Clinical characteristics at diagnosis in 75 *FLT3*-ITD positive AML patients with respect to response (relapse / refractory) and treatment (midostaurin / no midostaurin)

Variable	**Midostaurin-treated**			**Control**	
	Relapsed (n=35)	Refractory (n=19)	*P* Relapsed *vs* refractory	Relapsed (n=21)	*P* Relapsed midostaurin *vs* control
Age, years **Median (range)**	52 (20–69)	52 (38-66)	.59	52 (23–71)	.94
Sex, n (%) **Male** **Female**	24 (69) 11 (31)	6 (32) 13 (68)	**.01**	7 (33) 14 (67)	**.01**
AML history, n (%) ***de novo*** **sAML** **tAML**	33 (94) 1 (3) 1 (3)	16 (84) 3 (16) 0 (0)	.17	21 (100) 0 (0) 0 (0)	.54
Cytogenetics, n (%) **Normal karyotype** **Other** **Not available**	25 (71) 7 (20) 3 (0)	11 (58) 7 (37) 1 (5)	.20	18 (86) 3 (14) 0 (0)	.72
Leucocytes, x10^9/l* **Median (range)**	48 (2-304)	32 (2-251)	.40	35 (6-253)	.53
Blasts BM, %** **Median (range)**	88 (35–100)	83 (57-99)	.18	90 (31–95)	.75
Blasts PB*, %** **Median (range)**	48 (0–98)	76 (22-98)	.33	68 (0–94)	.17
Induction cycles, n (%) **1** **2**	25 (71) 10 (29)	15 (79) 4 (21)	.74	10 (48) 11 (52)	.09
Consolidation, n (%) **HDAC** **Allogeneic HSCT in CR1**	26 (74) 9 (26)	19 (100) 0 (0)	*ND*	19 (90) 2 (10)	.18
Midostaurin maintenance **Patients, n (%)** **Cycles, median (range)**	23 (43) 8 (1–12)	0 (0)	*ND*	0 (0)	*ND*
Time from diagnosis to refractory disease/relapse **Days, Median (range)**	324 (74–1451)	21 (39-84)	**<.0001**	253 (121 – 1339)	.41

*Not available (NA) in 5 patients **NA in 1 patient; ***NA in 6 patients; ****NA in refractory patients; n=number; BM=bone marrow; PB=peripheral blood; sAML=secondary AML; tAML=therapy-related AML; HDAC=High-dose cytarabine; HSCT=hematopoietic stem cell transplantation; CR1=first complete remission

Supplemental Table 3. Characteristics of *FLT3*-ITD clones detected at diagnosis and disease progression in midostaurin-treated patients with respect to gender

	All patients (n=54)		*P* Male vs female	Relapse patients (n=35)		*P* Male vs female	Refractory patients (n=19)		*P* Male vs female
Sex n (%)	Male 30 (56)	Female 24 (44)		Male 24 (69)	Female 11 (31)		Male 6 (32)	Female 13 (68)	
***FLT3*-ITD AR** Median (range)	0.46 (0.1-4.3)	0.54 (0.05-0.9)	.56	0.41 (0.06-0.9)	0.62 (0.1-1)	.69	.56 (0.5-4.3)	.51 (0.05-0.8)	.39
***FLT3*-ITD nt length** Median (range)	57 (21-225)	45 (21-102)	.31	54 (21-225)	41 (21-72)	.08	58 (21-99)	54 (27-102)	1
***FLT3*-ITD status at disease progression** Loss *FLT3*-ITD, n (%) Persistence *FLT3*-ITD, n (%)	 12 (40) 18 (60)	 13 (54) 11 (46)	.41	 12 (50) 12 (50)	 5 (45) 6 (55)	1	 0 (0) 6 (100)	 8 (62) 5 (38)	**.02**

AR=Allelic Ratio; n=number; *P*=p-value; NA=not available; ND=not determined; nt=nucleotide

Supplemental Table 4. Characteristics of all *FLT3*-ITD clones detected at diagnosis and disease progression in only relapsed midostaurin-treated patients and the control group

Variable	**Midostaurin (n=35)**			**No midostaurin (n=21)**			**Midostaurin *vs* control**	
	Diagnosis	**Disease progression**	***P***	**Diagnosis**	**Disease progression**	***P***	***P*** **Diagnosis**	***P*** **Progress**
Patients with multiple ITDs* **n (%)**	13 (37)	2 (6)	**.003**	4 (19)	2 (10)	.67	.23	.27
Total number of ITDs* **n**	51	21	*ND*	21	15	*ND*	*ND*	*ND*
***FLT3*-ITD AR** **Median** **(range)**	0.47 (0.06-0.99)	0.51 (0.07–26.31)	.96	.72 (0.05–18.94)	1.00 (0.05–38.75)	.28	.17	**.02**
FLT3*-ITD nt length **Median** **(range)**	51 (18–225)	45 (18–114)	.86	33 (15–81)	30 (18–72)	.31	**.01**	**.01**
FLT3*-ITD insertion site								
JMD	31 (61)	12 (58)	.80	18 (86)	12 (80)	.65	**.05**	.28
JM-Z	22 (43)	7 (33)		15 (71)	9 (60)			
JM-S	1 (2)	0 (0)		0 (0)	0 (0)			
Hinge region	8 (15)	5 (24)		3 (14)	3 (20)			
TKD1	20 (39)	9 (42)		3 (14)	3 (20)			
Beta1-sheet	20 (39)	6 (40)		3 (14)	3 (20)			
Nucleotide binding loop	0 (0)	0 (0)		0 (0)	0 (0)			
***FLT3*-ITD status at disease progression**								
***FLT3*-ITD positive**	26 (100)	18 (51)	*ND*	21 (100)	17 (81)	*ND*	*ND*	**.04**
No ITD detectable	*NA*	17 (49)	*ND*	*NA*	4 (19)	*ND*		

AR=Allelic Ratio; n=number; *P*=p-value; NA=not available; ND=not determined; nt=nucleotide; JMD=juxtamembrane domain; TKD=tyrosine kinase domain. *Data available for n=18 patients at diagnosis and n=17 patients at relapse in the control group

Supplemental Table 5. Median p-FLT3 levels of n=12 midostaurin-treated patients after 1st Induction chemotherapy and at relapse / refractory disease

	All patients (n=12)	***FLT3*-ITD positive at disease progression (n=6)**	***FLT3*-ITD negative at disease progression (n=6)**	***P*** ***FLT3* positive *vs* negative**
End of 1st Induction % p-FLT3 level median (range)	31 (14-93)	41 (20-93)	31 (14-88)	.59
Relapse / Refractory % p-FLT3 level median (range)	59 (20-100)	51 (20-100)	65 (39-100)	.62
P **End of Induction *vs* disease progression**	.08	.73	**.05**	

p-FLT3=phosphorylated FLT3

Supplemental Table 6. Genes included in the validation platform for ultra-deep targeted-resequencing of recurrently mutated genes in AML

Genes			
ANKRD26	ETV6	MPL	SMC1A
ASXL1	EZH2	MYC	SRSF2
ASXL2	FLT3	NF1	STAG2
BCOR	GATA2	NPM1	TET2
BRAF	IDH1	NRAS	TP53
CALR	IDH2	PHF6	U2AF1
CBL	JAK2	PPM1D	WT1
CEBPA	KDM6A	PTPN11	ZBTB7A
CSF3R	KIT	RAD21	ZRSR2
DDX41	KRAS	RUNX1	
DNMT3A	MLL (KMT2A)	SF3B1	

Supplemental Table 7. Presence of recurrent gene mutations at diagnosis and relapse detected with ultra-deep sequencing in selected midostaurin-treated patients (n=3)

UPN	*FLT3*-ITD at relapse	Gene	Variant	AA change	VAF (%) diagnosis	VAF (%) relapse
43	negative	DNMT3A	NM_175629:exon15:c.G1685A	p.C562Y	49.44	49.49
43	negative	U2AF1	NM_006758:exon2:c.C101T	p.S34F	46.46	44.56
43	negative	FLT3	NM_004119:exon20:c.G2503T	p.D835Y	19.58	ND
43	negative	NRAS	NM_002524:exon2:c.G35A	p.G12D	7.78	ND
43	negative	WT1	NM_000378:exon7:c.1283_1284insGACA	p.H428fs	23.08	ND
43	negative	BCOR	NM_017745:exon4:c.G2166C	p.L722F	ND	6.85
43	negative	KRAS	NM_033360:exon2:c.G38A	p.G13D	ND	11.76
29	negative	TET2	NM_017628:exon3:c.822delC	p.I274fs	42.39	33.87
29	negative	NRAS	NM_002524:exon2:c.G35C	p.G12A	19.50	41.84
29	negative	RUNX1	NM_001754:exon5:c.C480A	p.D160E	ND	29.09
16	positive	WT1	NM_024426:exon7:c.1140_1141insCTCTTGTACGG	p.S381fs	51.29	32.61
16	positive	WT1	NM_024426:exon7:c.1144_1145insTCGG	p.A382fs	63.32	22.42
16	positive	ASXL1	NM_015338:exon12:c.G3306T	p.E1102D	ND	4.49
16	positive	ZBTB7A	NM_015898:exon2:c.C1204T	p.R402C	ND	30.03

AA=Amino acid; ND=not detected; VAF=Variant Allele Frequency

Supplemental Figures

Supplemental Figure 1. Presence of *FLT3*-ITD clones at diagnosis and disease progression based on a Genescan-based routine diagnostic assay in midostaurin-treated patients. (A) Presence of *FLT3*-ITD clones at diagnosis (D) and relapse (R); (B) presence of *FLT3*-ITD clones at D and refractory disease. Each column represents one patient. Green indicates that the same ITDs were detected at both time points. A change of the ITD between D and disease progression is color-coded in orange (light: loss of ITD at progression with at least 1 persistent *FLT3*-ITD clone between both time points; medium: switch of ITD insertion site or ITD length; dark: gain of ITD clone at R). Blue indicates that no *FLT3*-ITDs were detected at disease progression.

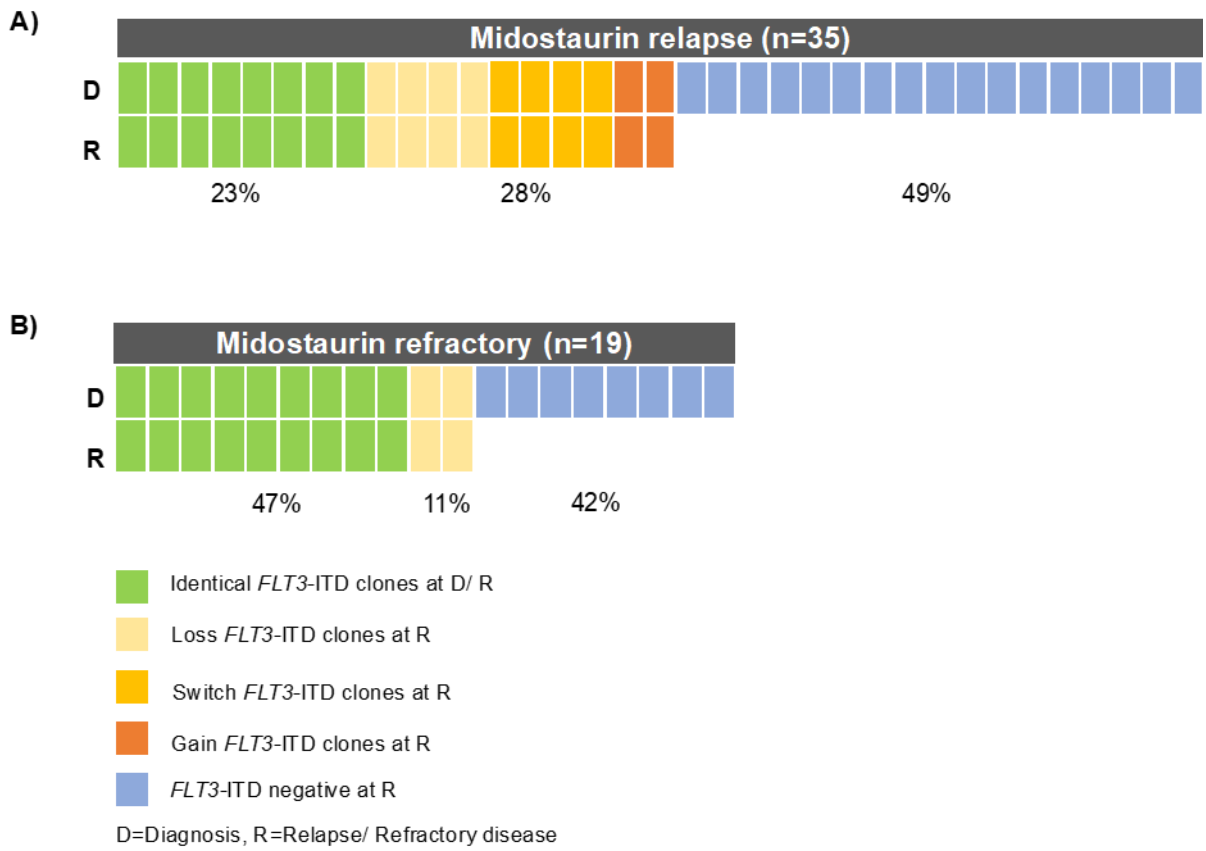

Supplemental Figure 2A. Somatic variants detected with WES in relapsed / refractory patients. Given is the number and percentage of mutations detected exclusively at diagnosis (blue), in midostaurin-treated patients exclusively at relapse (red) or refractory disease (green) as well as in the control group at disease progression (grey). Numbers in the intersections represent mutations that were present at both time points.

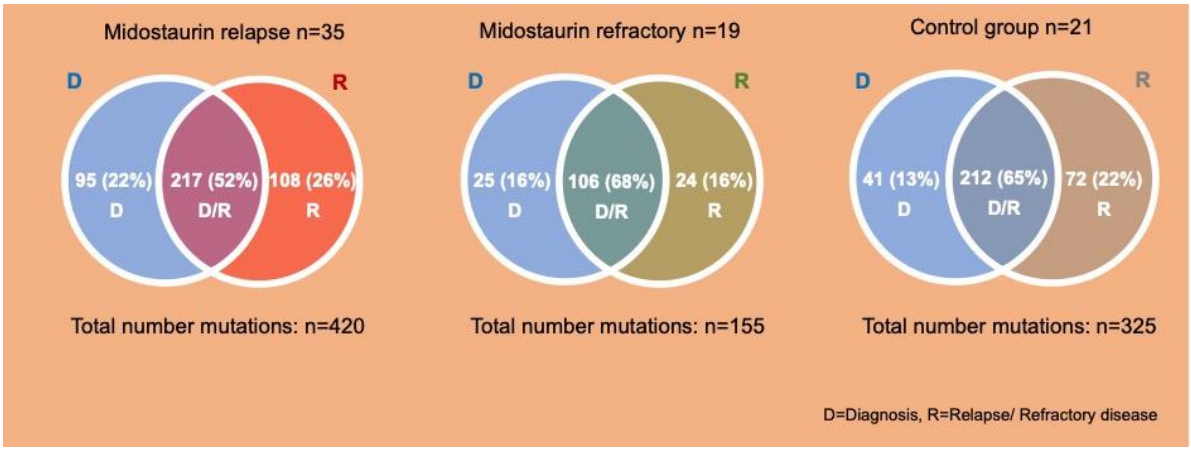

Supplemental Figure 2B. Median number of mutations in relapsed / refractory midostaurin-treated patients present at the time of diagnosis (blue), relapse (red) or refractory disease (green). Each dot represents the number of mutations found in a given patient at a given time point. P values were calculated using the Mann-Whitney test.

Midostaurin relapse (n=35)

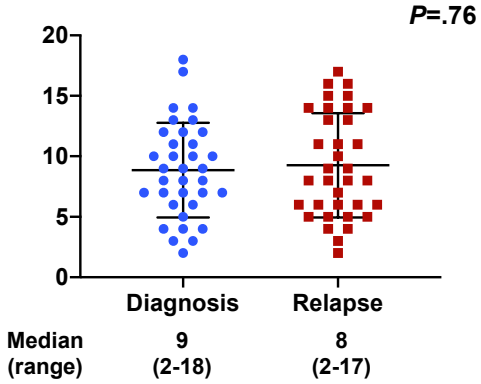

Midostaurin refractory (n=19)

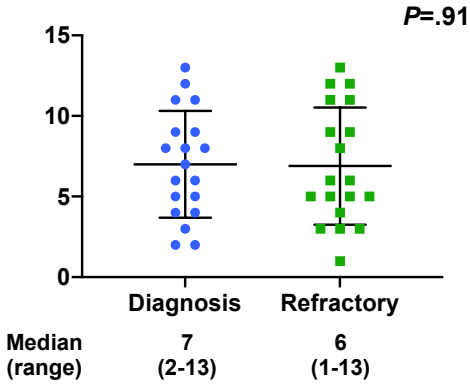

Supplemental Figure 2C. Stability of mutations in midostaurin-treated patients between diagnosis and relapse / refractory disease. Each bar represents one patient. Given is the percentage of mutations present at diagnosis (blue), at relapse (red) / refractory disease (green) and present at both time points (yellow). Bars are arranged in descending order of stable mutations (yellow). The presence of *FLT3*-ITD (+/-) at relapse / refractory disease is given on the top of each bar.

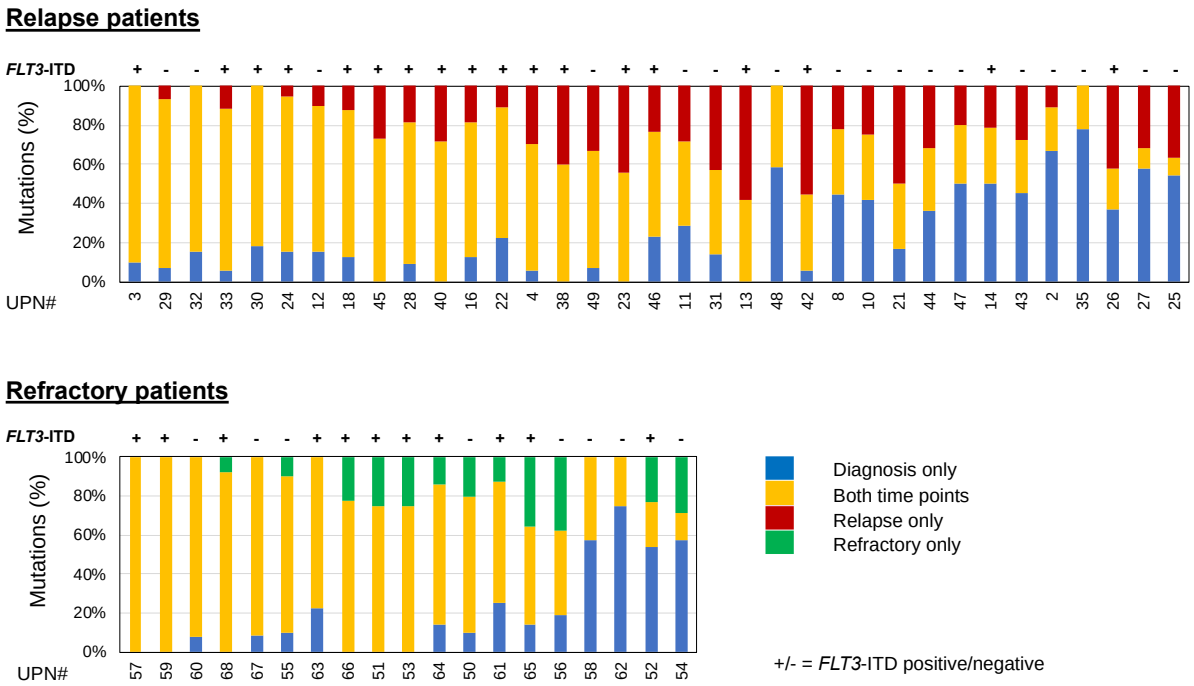

Supplemental Figure 3. Classification of relapse and refractory disease patients treated with midostaurin according to genomic groups.[17] Bars indicate the number of patients assigned to a genomic group (grey: relapse / refractory disease patients; blue: refractory disease patients; red: patients with relapsed disease).

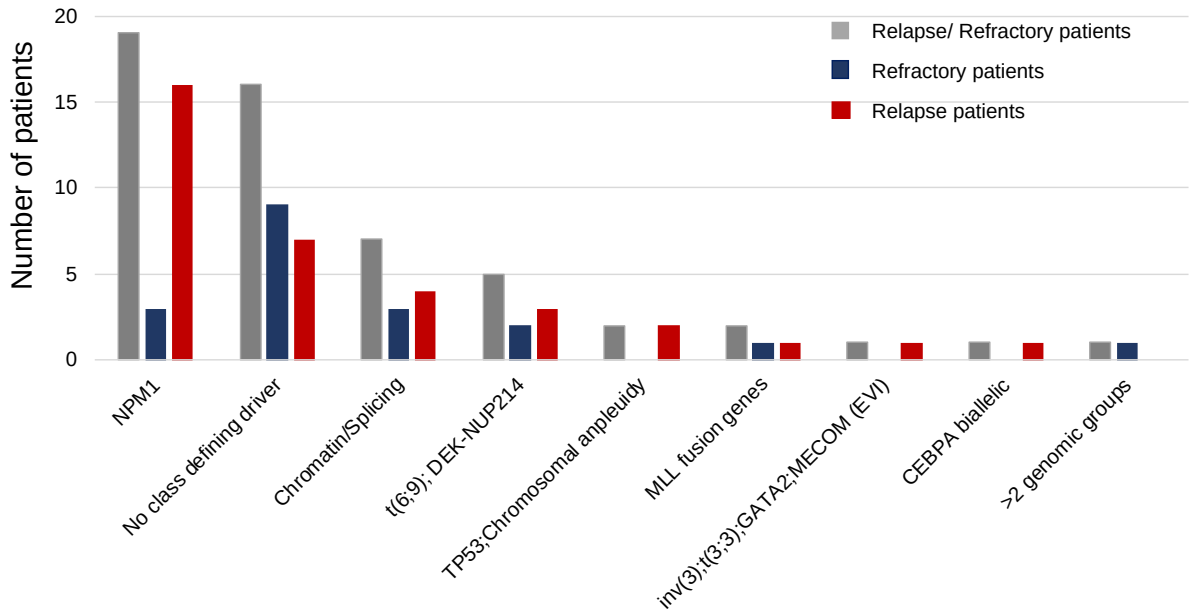

Supplemental Figure 4A. Frequencies of recurrent gene mutations in relapse (n=35; top) and refractory disease (n=19; bottom) patients treated with midostaurin. Genes are arranged according to functional groups as described above the graph. Mutations present only at diagnosis are color-coded in blue, detected only at relapse / refractory disease in red, and at both time points in yellow.

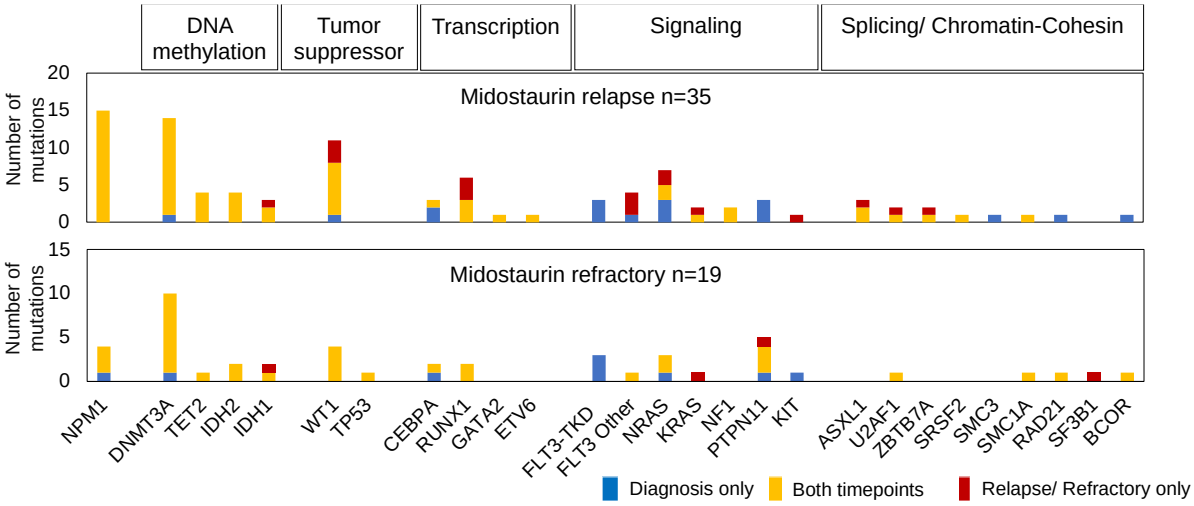

Supplemental Figure 4B. Presence of gene mutations in midostaurin-treated relapsed (left) and refractory disease (right) patients. Genes are arranged according to functional groups. Each column represents one single patient. For each patient, the presence of a mutation is given at diagnosis and relapse / refractory disease in subsequent rows. Blue indicates the presence of a mutation (grey = wildtype). Mutations present only at relapse / refractory disease are highlighted in red. The number (n) and percentage (%) of mutations at the respective time points are given next to the figures.

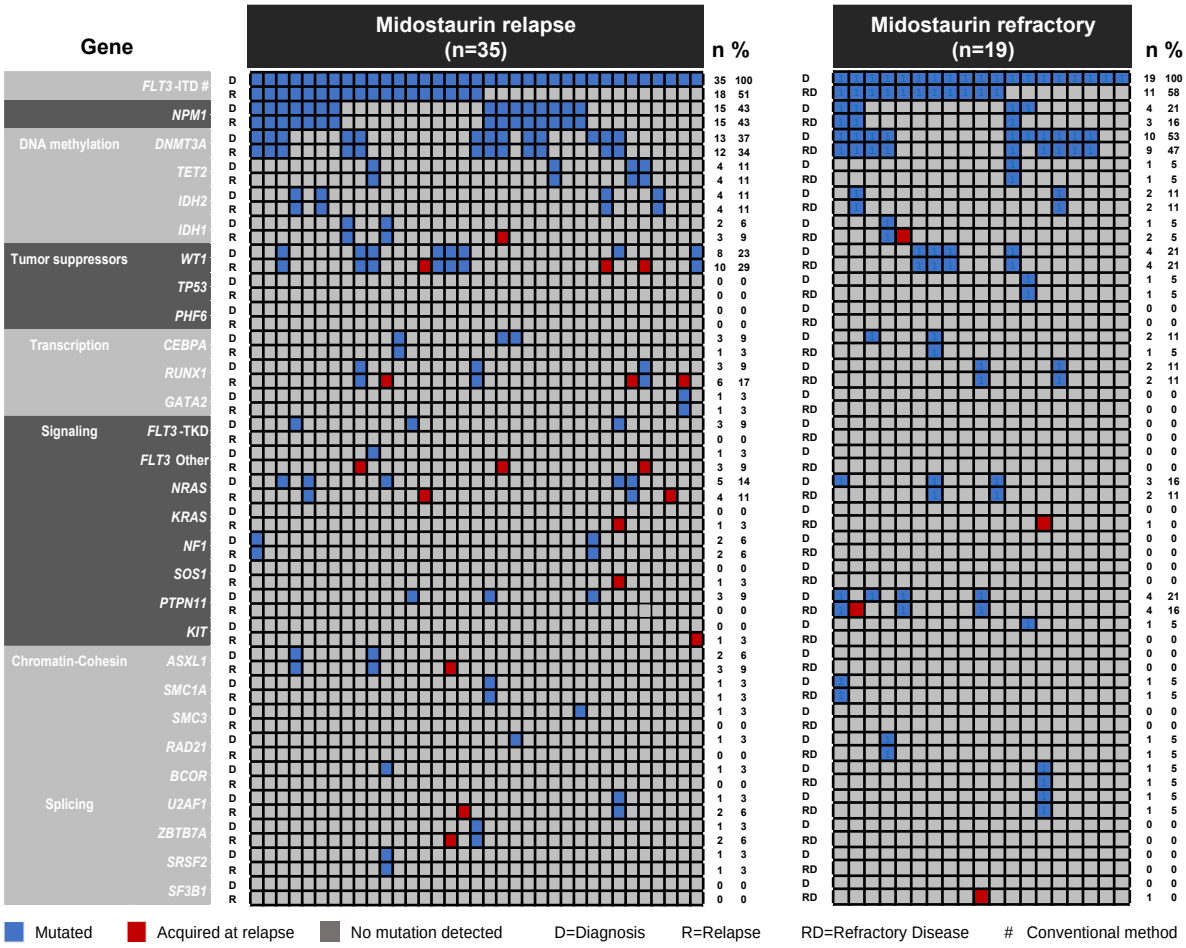

Supplemental Figure 5A. Gene enrichment analysis at the time of diagnosis between relapsed and refractory disease patients treated with midostaurin. Given are genes that were enriched in KEGG pathways. Gene names are given at the left of each row, KEGG gene sets at the top of each column. The presence of mutations is indicated in blue (grey = no mutation). The black frame highlights different gene cluster between relapsed and refractory patients.

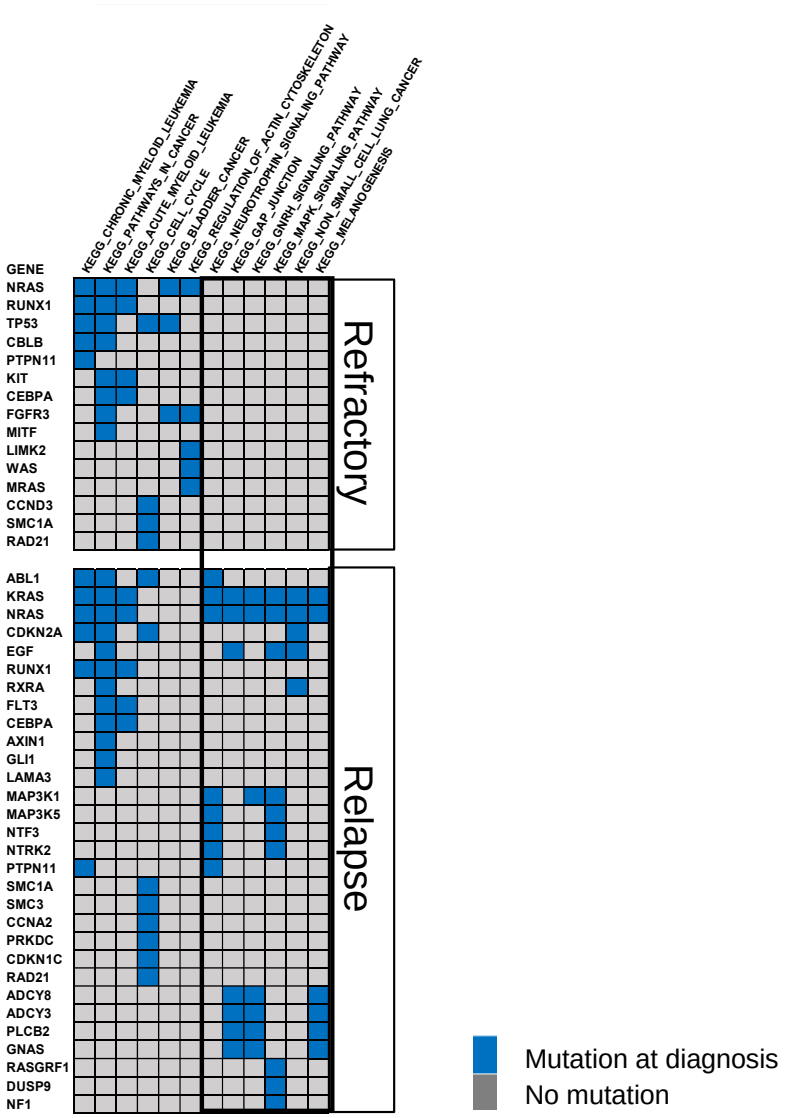

Supplemental Figure 5B. Gene enrichment analysis in midostaurin-treated patients between diagnosis and relapse / refractory disease. Depicted are genes that were enriched in KEGG pathways. Gene names are given at the left of each row, KEGG gene sets at the top of each column. The presence of mutations is indicated in blue (grey=no mutation).

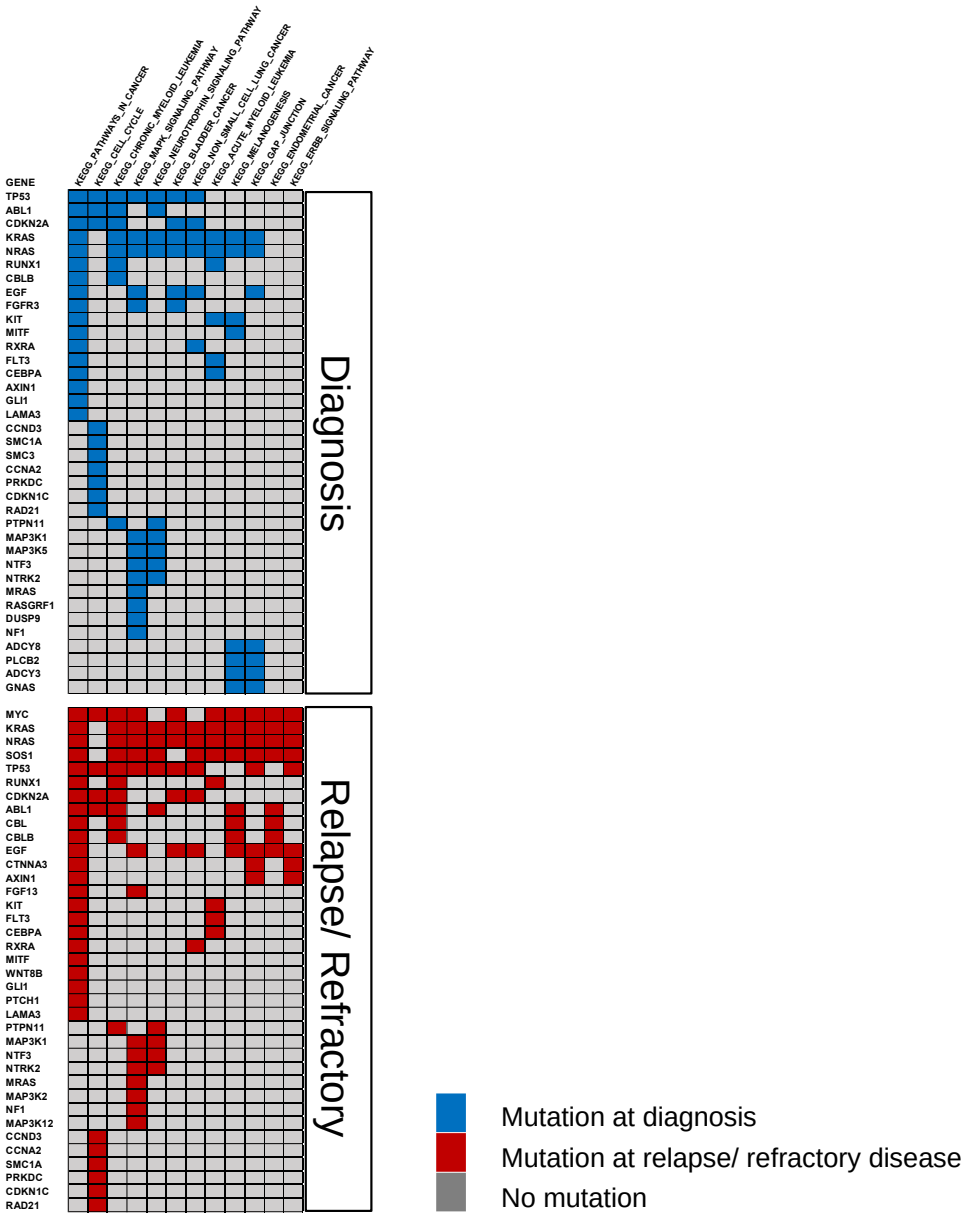

Supplemental Figure 5C. Gene enrichment analysis in midostaurin-treated patients at diagnosis (left) and relapse / refractory disease according to *FLT3*-ITD status at disease progression. Depicted are genes that were enriched in KEGG pathways. Gene names are given at the left of each row, KEGG gene sets at the top of each column. The presence of mutations is indicated in blue (grey = no mutation). The black frame highlights different gene cluster between *FLT3*-ITD positive and negative patients.

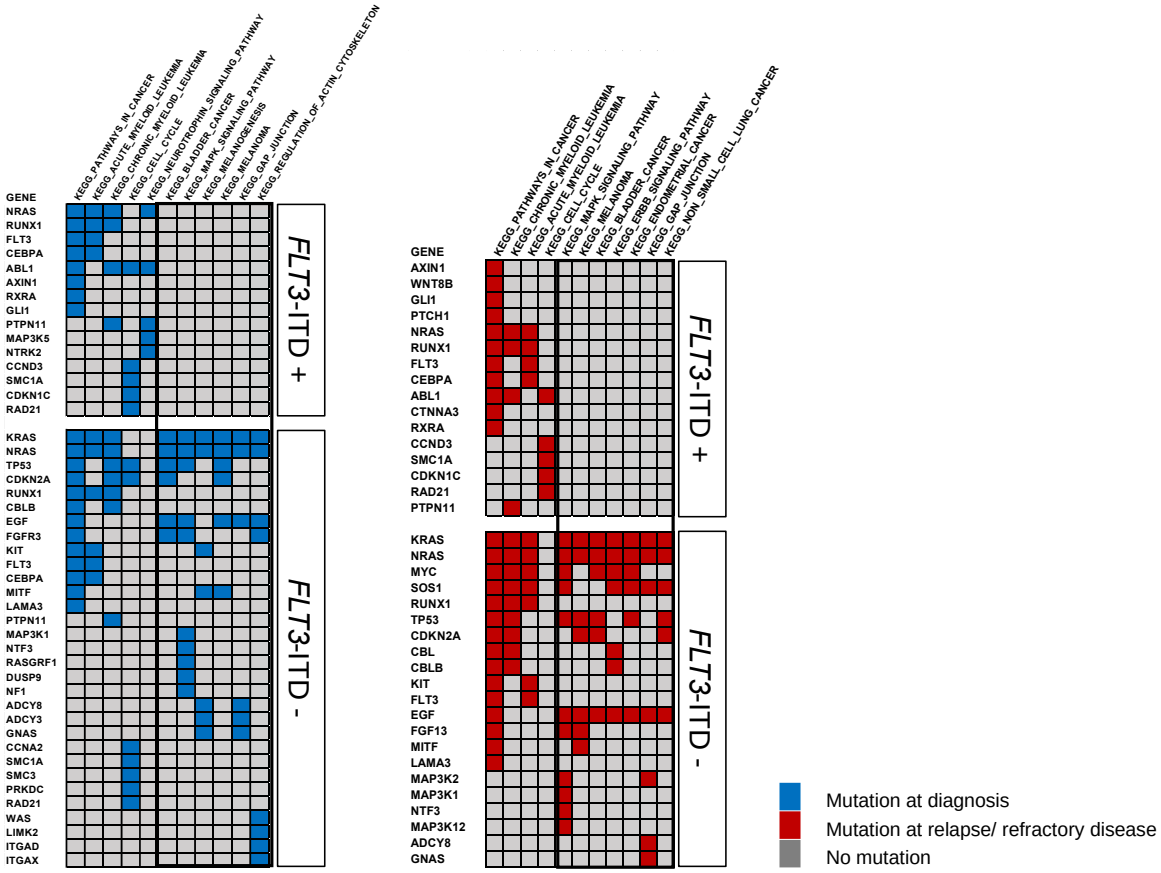

Supplemental Figure 6. Clonal evolution of 2 patients with negative *FLT3*-ITD at relapse and persisting pre-leukemic mutations in complete remission.

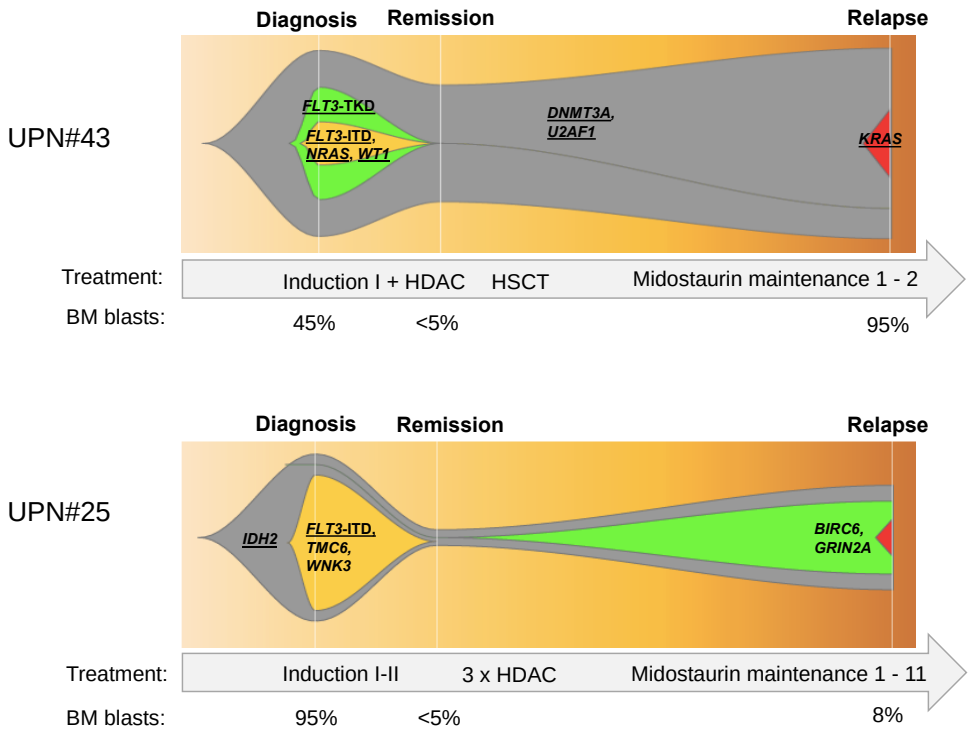

HDAC=high-dose cytarabine
BM=bone marrow
HSCT=hematopoietic stem cell transplantation

Supplemental Figure 7. Fish plot visualization of different patterns of clonal evolution in 4 patients with refractory disease (three patients were considered refractory following one cycle of induction therapy, “Induction I”, and one patient following two cycles, “Induction II”). While in patients UPN#54 (A) and UPN#67 (B) the *FLT3*-ITD mutant clone was eradicated during induction therapy and did not account for the refractory disease, in patients UPN#59 (C) and UPN#56 (D) the *FLT3*-ITD mutant clone persisted at disease progression.

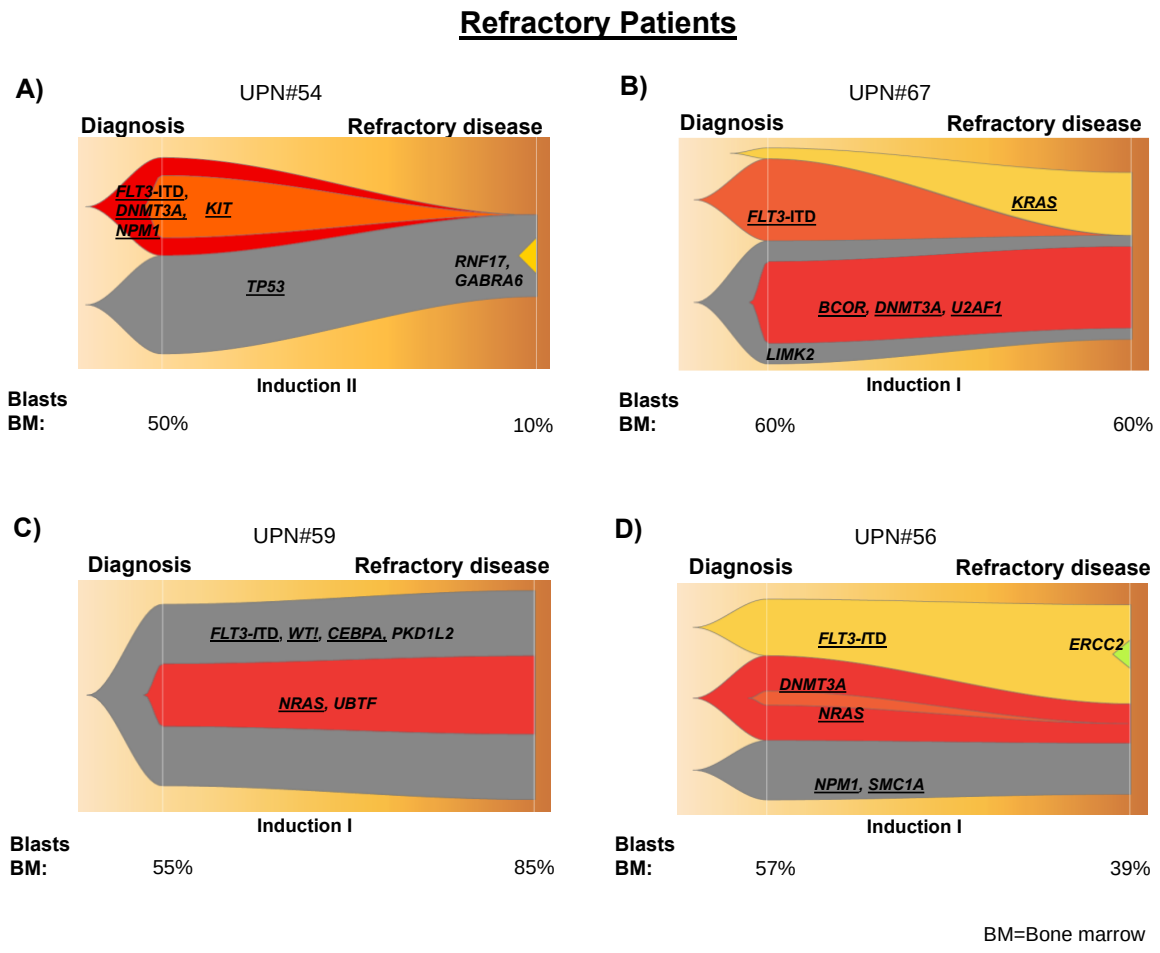

Supplemental Figure 8. Graphs show the plasma inhibitory activity (PIA) of midostaurin during the course of treatment in two relapse (UPN#13 and #16) and two refractory (UPN#57 and #53) patients with positive *FLT3*-ITD at relapse / refractory disease. PIA is reflected by the mean phosphorylated (p) FLT3 levels ranging between 0 and 100%. A p-FLT3 level of 100% means no FLT3-inhibition. The clonal evolution of mutations at the respective time points is depicted as fish plots below the graphs. (Ind=Induction, Cons=consolidation, HSCT=hematopoietic stem cell transplantation, CR=complete remission).

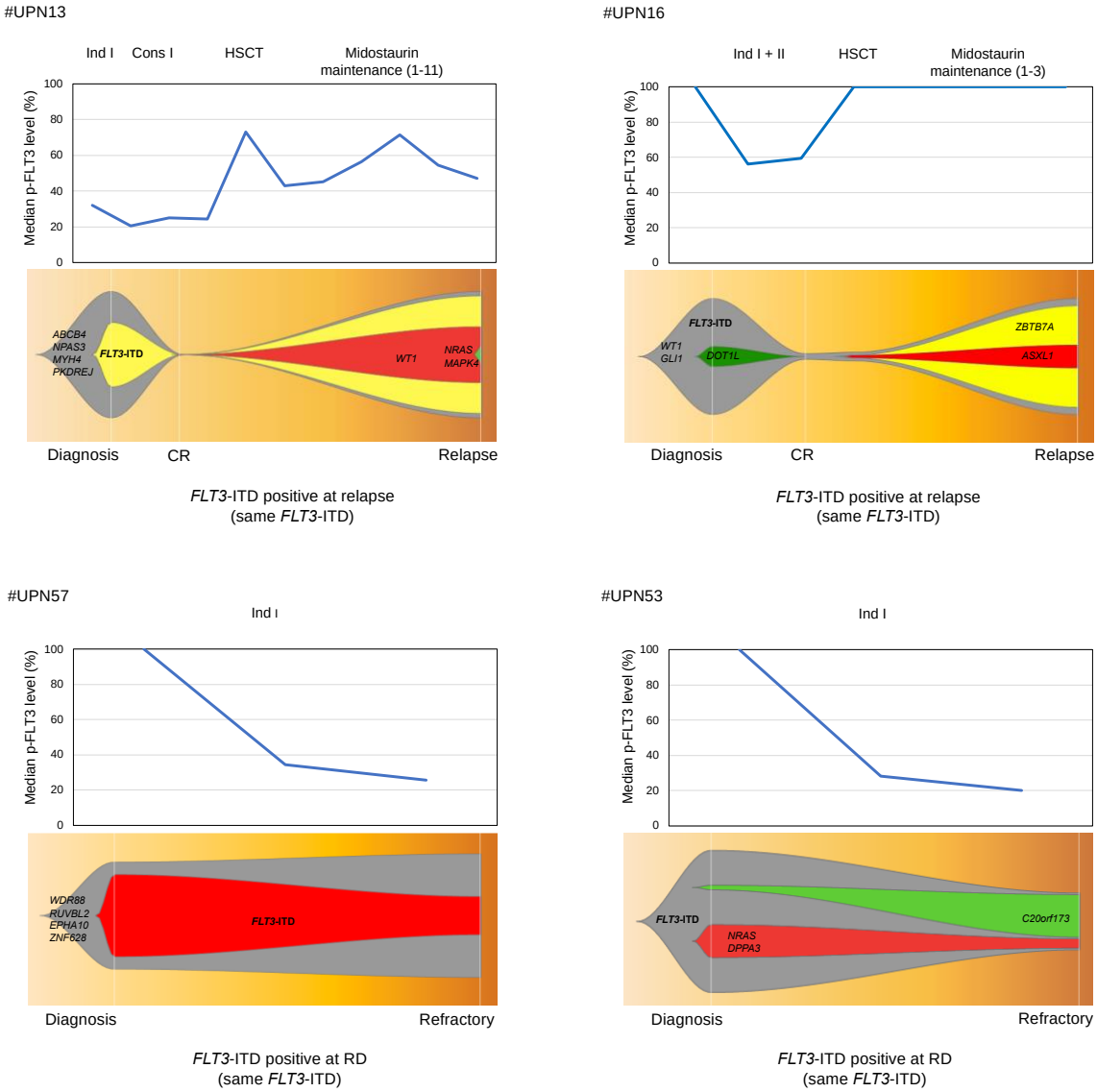
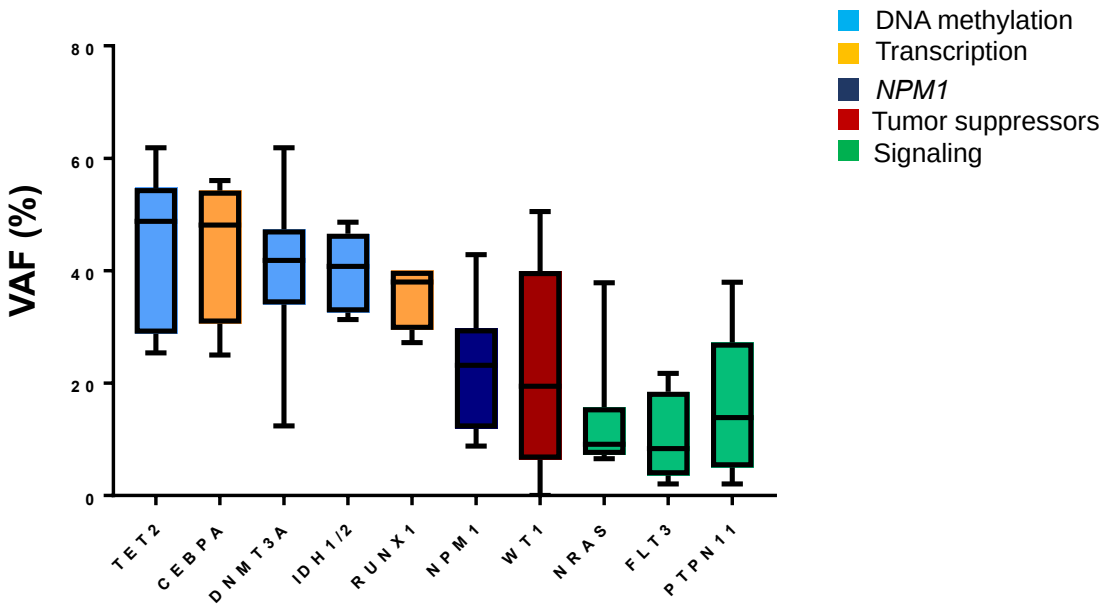
Supplemental Figure 9. Variant allele frequencies (VAFs) at diagnosis according to genes and functional groups. Box-plots show the median VAFs (%) among all mutations, whiskers reflect minimal and maximal values. In line with previous findings, these data indicate that epigenetic driver mutations, which are frequently associated with clonal hematopoiesis, usually represent early genetic events with mutations being present in almost all malignant cells with VAF ~50%; whereas mutations in signaling genes are often subclonal events occurring at a later stage of the disease evolution.